

Modelling hadron-hadron Interactions: from Particle Physics at Colliders to Cosmic Ray Physics

Maria Vittoria Garzelli

e-mail: garzelli@mi.infn.it

University of Nova Gorica, Laboratory for Astroparticle Physics,
April 18th, 2011

Abstract

Understanding the **multiple aspects** of the **physics of h-h interactions** is crucial for both data analysis at recent colliders like Tevatron and LHC and for the simulation of Cosmic Ray interactions in the Earth's atmosphere. In this talk I will review the status of the theory behind MC codes used in both cases, by distinguishing between **hard** and **soft collision processes** and by giving a point of view, far from being complete, built on the basis of my working experience in the **Helac-NLO** and the **FLUKA** collaborations.

Hadrons

- **Hadrons** are **composite objects**, made by **partons**, i.e. **quarks** and **gluons**. We can distinguish:
 - **mesons** ($q\bar{q}$): π , K , etc...
 - **baryons** (qqq): n , p , etc....
 - **antibaryons** ($\bar{q}\bar{q}\bar{q}$): \bar{n} , \bar{p} , etc....
- **Gluons** are **colored partons** (8 possible color combinations), as well as quarks (3 possible colors). **Hadrons are color singlets**.
- The **gluons** act as a **“glue”** between **quarks**, keeping mesons and baryons **confined**.
- Hadron properties are listed in the Particle Data Book(let).

Hadronic interactions: h - h, h - A and A - A

h - h interactions:

- **hard component**: Q large, small impact parameter
- **soft component**: Q small, large impact parameter

Both components are present in CR interactions in the atmosphere and in p - p scatterings at LHC and are described by means of **QCD**, the theory of strong interactions. However, the hard component is more interesting for LHC physics, and the soft one for CR physics.

* $\alpha_S \rightarrow +\infty$ for $Q \rightarrow 0$ (**confinement**).

* $\alpha_S \rightarrow 0$ for $Q \rightarrow \infty$ (**asymptotic freedom**).

pQCD: quantum field theory, perturbative expansion in the α_S coupling constant. Valid only if $\alpha_S \ll 1$, i.e. if Q is large enough ($\Lambda_{QCD} \sim 1\text{GeV}$).

\Rightarrow **pQCD**, that is a theoretically well founded and elegant approach, **can be used to describe only the hard component** of h - h interactions, but **fails in the description of the soft one!**

QCD: α_s determination at Tevatron

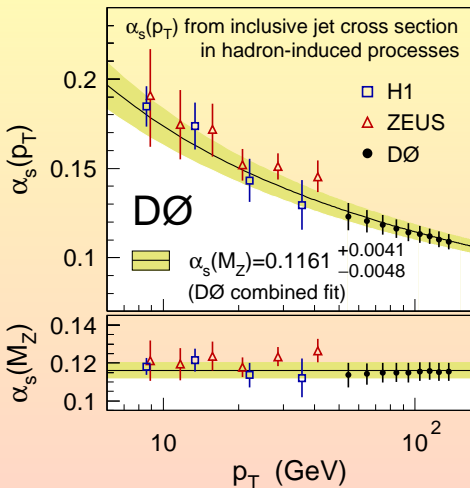


Figure: The strong coupling constant α_s as a function of p_T (top) and at M_Z (bottom). For comparison HERA DIS jet data are superposed. Error bars correspond to total uncertainties. (Figure taken from L. Sonnenschein on behalf of the D0 collab., arXiv:1006.2855[hep-ex])

pQCD: basic ingredients

gluons, quarks, ghosts and their interactions:

$$\frac{p}{\mu, a} \begin{array}{c} \text{---} \\ \text{---} \\ \text{---} \\ \text{---} \\ \text{---} \\ \text{---} \\ \text{---} \\ \text{---} \end{array} \nu, b = -i \frac{g_{\mu\nu}}{p^2} \delta_{ab}, \quad \frac{p}{l} \text{---} k = \frac{i \delta_{kl}}{\not{p} - m_q}, \quad \text{---} \frac{p}{a} \text{---} b = \frac{i \delta_{ab}}{p^2},$$

$$\begin{array}{c} \mu_2, a_2 \\ \swarrow \\ \text{---} \\ \swarrow \\ \mu_1, a_1 \end{array} \begin{array}{c} p_1 \\ \text{---} \\ \text{---} \\ \text{---} \\ \text{---} \\ \text{---} \\ \text{---} \\ \text{---} \end{array} \begin{array}{c} p_2 \\ \swarrow \\ \text{---} \\ \swarrow \\ \mu_3, a_3 \end{array} = g f^{a_1 a_2 a_3} V_{\mu_1 \mu_2 \mu_3}(p_1, p_2, p_3),$$

$$\begin{array}{c} \mu, a \\ \swarrow \\ \text{---} \\ \swarrow \\ \sigma, d \end{array} \begin{array}{c} \nu, b \\ \swarrow \\ \text{---} \\ \swarrow \\ \rho, c \end{array} = -ig^2 [f^{ebc} f^{eda} (g_{\nu\sigma} g_{\mu\rho} - g_{\mu\nu} g_{\rho\sigma}) + f^{ebd} f^{eac} (g_{\mu\nu} g_{\rho\sigma} - g_{\nu\rho} g_{\mu\sigma}) + f^{eba} f^{ecd} (g_{\nu\rho} g_{\mu\sigma} - g_{\nu\sigma} g_{\mu\rho})],$$

$$\begin{array}{c} k \\ \swarrow \\ \text{---} \\ \swarrow \\ \mu, a \end{array} = -igt^a \gamma^\mu,$$

$$\begin{array}{c} p \\ \swarrow \\ \text{---} \\ \swarrow \\ \mu, c \end{array} = gf^{abc} p_\mu,$$

$$\begin{array}{c} k \\ \swarrow \\ \text{---} \\ \swarrow \\ V \\ \mu \end{array} = \delta_{kl} \gamma_\mu (v + a \gamma_5)$$

$$\begin{array}{c} k \\ \swarrow \\ \text{---} \\ \swarrow \\ S \end{array} = \delta_{kl} (c + d \gamma_5)$$

Figure: Feynman rules used for the computation. The last two vertices parametrize a generic coupling of a (pseudo)-vector V and of a (pseudo)-scalar S with a quark line, respectively. (Figure taken from P. Draggotis, M.V.G., C. Papadopoulos, R. Pittau, JHEP 0904 (2009), 072)

Factorisation theorem cartoon

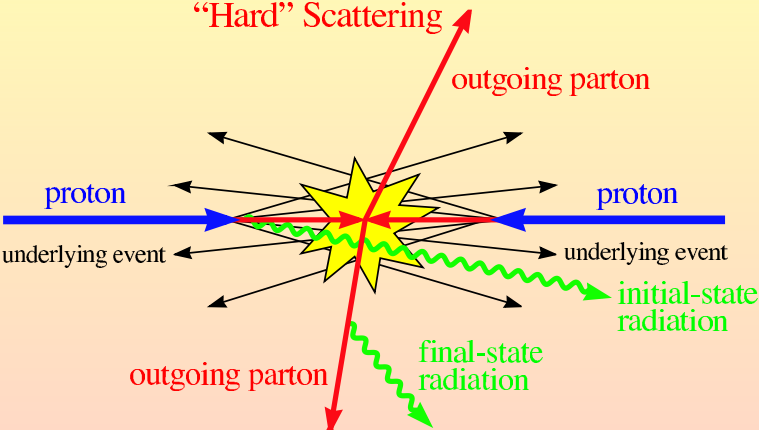


Figure: Schematic cartoon of a $2 \rightarrow 2$ hard scattering event. (Figure taken from J.M. Campbell, J. Huston, W.J. Stirling, Rept. Prog. Phys. 70 (2007), 89)

h - h interactions (from a collider physicist point of view...)

Factorisation Theorem: each h - h interaction can be factorized (i.e. decomposed) in parts, each one characterized by a different energy scale:

1) the **hard-scattering** event, involving two partons, one from each hadron ($E_{CM} = \sqrt{s}$). In general, only one hard-scattering event for each h - h scattering at accelerators is considered, but more than one (hard or semi-hard) are possible (beyond factorisation effect, see e.g. recent work at Argonne Univ.)

2) the **parton shower (PS)** phase: gluons and light quarks in the initial and final states further radiate softer gluons and quarks, giving rise to a cascade. One speaks about Initial State Radiation (ISR) and Final State Radiation (FSR).

n.b. the top quark (heavy! $m_t \sim 173\text{GeV}$), due to its typical life-time, in general decays before radiating lighter particles.

3) the **underlying event**, allowing to describe the fate of the “spectator” partons, not involved in the hard-scattering (non-perturbative effect).

4) the **hadronisation** phase ($E \sim \text{a few } \Lambda_{QCD}$): final state quarks and gluons combine together in hadrons, impinging on the detectors (eventually, after a **decay**).

Each of these stages can in general be described by a **MC code**. The interfaces between different phases (i.e. the **output** of each MC) are or are going to be **standardized** (\rightarrow see the **Les Houches accords**).

\Rightarrow This allows to use different combinations of MCs interfaced together.

A pictorial representation: a $p - \bar{p}$ collision

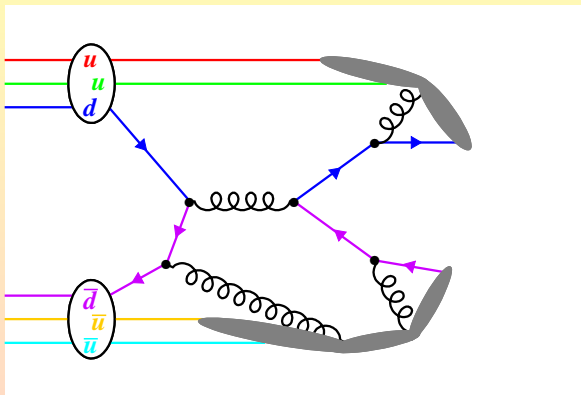


Figure: A drawing, illustrating jet production in a $p - \bar{p}$ collision with the hard scattering process, initial state, final state radiation and hadronisation (jet fragmentation) including the underlying event. (Figure taken from L. Sonnenschein on behalf of the D0 collab., arXiv:1006.2855v1[hep-ex])

Another pictorial representation: a p-p collision

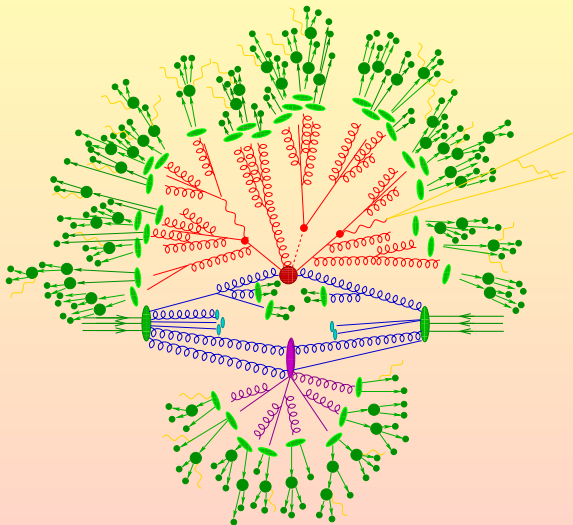


Figure: The hard interaction (big red blob) is followed by the decay of both top quarks and the Higgs boson (small red blobs). Additional hard QCD radiation is produced (red) and a secondary interaction takes place (purple blob) before the final-state partons hadronise (light green blobs) and hadrons decay (dark green blobs). Photon radiation occurs at any stage (yellow). (Figure taken from T. Gleisberg et al., JHEP 02 (2009), 007)

1) The hard scattering event


At present, different MC codes allow to describe hard scatterings. They have been primarily designed for accelerator physics.

The user typically selects an input process ($p-p$, $p-\bar{p}$, e^+e^-), then the code takes care of decomposing it in all possible subprocesses ($q-\bar{q}$, $q-g$, $g-g$, *etc...*), of computing the matrix element for each of them, for all possible helicity and color configurations, integrating the squared module over the available phase-space and summing all contributions together. The phase-space is indeed specified by the user by means of cuts allowing to reproduce the experimental conditions (and, eventually, screening the divergences at LO).

Matrix elements are computed at a fixed order in perturbation theory by means of pQCD (and eventually the EW perturbative theory completing the $SU(3)_C \times SU(2)_W \times U(1)_Y$ Standard Model of elementary particle interactions).

QCD factorization:

$$d\sigma_{H_1 H_2 \rightarrow X} = \sum_{i,j} \int dx_1 dx_2 f_{i/H_1}(x_i, \mu_F) f_{j/H_2}(x_j, \mu_F) \int d\phi |\mathcal{M}_{ij \rightarrow X}(x_i p_1, x_j p_2, \alpha_S(\mu_R), \mu_F)|^2$$

valid if hard scattering scale \gg hadronisation scale $\sim 1\text{GeV}$. 

Hadron-Hadron cross section

QCD factorization:

$$d\sigma_{H_1 H_2 \rightarrow X} = \sum_{i,j} \int dx_1 dx_2 f_{i/H_1}(x_i, \mu_F) f_{j/H_2}(x_j, \mu_F) d\hat{\sigma}_{ij \rightarrow X}(x_i p_1, x_j p_2, \alpha_S(\mu_R), \mu_F)$$

valid if hard scattering scale \gg hadronisation scale $\sim 1 \text{ GeV}$

- * μ_F factorization scale (IR origin)
- * μ_R renormalization scale (UV origin)
- * $f_{i,j}$ parton distribution functions
- * $\hat{\sigma}_{ij}$ partonic cross-section, on the basis of the matrix element for the hard scattering process (at present LO matrix elements in many MC event generators, even for processes with many external legs, thanks to off-shell recursive relations)
- * σ in LO pert. theory has a logarithmic dependence on μ_R and μ_F

NLO is needed for reducing scale dependence uncertainties
(and non always enough...)

Why Monte Carlo methods are used ?

- MC integration over the (complicated) **phase-space**
- MC sum over **color** configurations (quarks and gluons are colored particles)
- MC sum over **helicity** configurations

⇒ The last two techniques (with respect to standard sums over all possible configurations) considerably **speed up** the computation.

First option: **Leading-Order (LO)** event generators

These were the first ones being developed. Many of them are freely available on the web ([MadGraph/MadEvent](#), [Alpgen](#), [Helac-Phegas](#), [CompHEP/CalcHEP](#), [SHERPA](#), [Whizard](#).....).

- They can be based on a **Feynman diagram** description, i.e. for each given subprocess, at fixed external legs, all contributing Feynman diagrams at fixed orders in the perturbative constants α_S and g_W are shown (e.g. the [MadGraph/MadEvent](#) MC).

Drawback: for a process with n external legs, the number of contributing Feynman diagrams is of the order of $n!$.

- A substantial progress was achieved with the introduction of **recursion relations** (~ 1994). By means of these mathematical equations it is possible to write down the amplitude corresponding to each subprocess **without writing down and computing all separated Feynman diagrams**. The mathematical complexity of the computation increases as $\sim 3^n$ instead of $n!$. \Rightarrow Advantage in case of **multiparticle final states** ($n \geq 6$). This is important at higher energies, where an increasing number of jets can appear.

Recursion relations are implemented in MC codes like [Alpgen](#) and [Helac](#).

The hard scattering event: radiative corrections

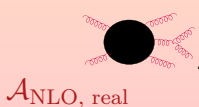
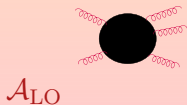
Second option: Next-to-Leading-order (NLO) event generators

Going to NLO is necessary in pQCD at present colliders, especially when studying states involving an high number of external particles, since

- it allows to reduce the dependence on unphysical scales (μ_F and μ_R), typical of LO results.
- Furthermore it allows to better determine the shapes of kinematical distributions (rapidity, p_T , invariant masses, etc.)

When going from LO to NLO, two kinds of radiative corrections appear:

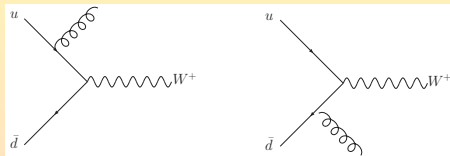
- virtual corrections (i.e. loops)
- real corrections, involving one (and only one) additional external leg with respect to the LO process (and no loops).



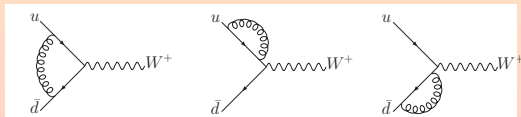
Real and virtual contributions: an example

NLO corrections to the Drell-Yan production of a W boson:

- Contributing **real diagrams**:



- Contributing **virtual diagrams**:



Figures from J.M. Campbell, J. Huston, Stirling, Rept. Prog. Phys. 70 (2007), 89

Divergences in the computation of radiative corrections

- **Ultraviolet** divergences ($p \rightarrow +\infty$) \Rightarrow reabsorbed through renormalization
- **Infrared** divergences
 - Soft singularities ($p \rightarrow 0$)
 - Collinear singularities ($\theta_{\text{emission}} = 0$) \Rightarrow cancel between real and virtual contributions for infrared-safe observables.

Virtual correction computation

At present NLO event generators are **under construction**. No one is already available on the web!

The difficulty arises from the fact that **divergences** in general appear in the computation of both the virtual and the real correction contributions.

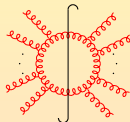
As for **virtual corrections**, each loop leads to the appearance of an **integral over the loop momentum** $\int d^4q$. Due to the appearance of divergences, the integral is performed in $d = 4 + \epsilon$ dimensions instead of in 4, and the limit $\epsilon \rightarrow 0$ is taken after (**dimensional regularization**).

The actual computation of such a kind of **tensorial integrals** can in general be cumbersome and time-consuming, even from the numerical point of view. The introduction of **alternative methods** to compute loop amplitudes, **inspired by unitarity and generalized unitarity** concepts, has led to important progresses in this field.

Unitarity methods

$$S = 1 + iT, \quad S^\dagger S = 1 \quad \Rightarrow \quad 2\text{Im}(T) = T^\dagger T$$

$$\Rightarrow \text{Im } \mathcal{A}^{1\text{-loop}} \sim \sum_{\text{cuts}} \int dPS_{\text{cut}}$$



- **Original Unitarity** formulation [Bern, Dixon, Dunbar, Kosower Nucl. Phys. B 425 (1994) 217]: **only 1** two-particle **cut**
- **Generalized Unitarity** [Britto, Cachazo, Feng Nucl. Phys. B 725 (2005) 275]: **multiple** (quadruple) **cuts**, first introduced in $\mathcal{N} = 4$ Super-Yang-Mills theories.

These developments have led to the construction of codes like **Helac-1-loop** and **MadLoop**, where each 1-loop contribution is obtained from tree-level diagrams, by cutting up to four loop propagators.

Example of virtual NLO correction computation

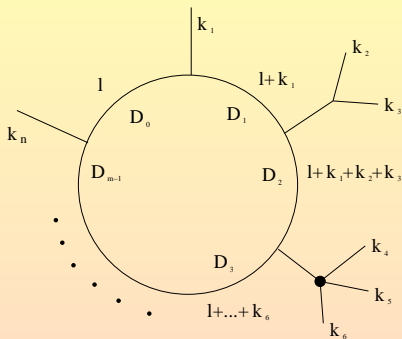


Figure: An n -point one-loop diagram with m propagators in the loop. The dark blob represents a tree structure. (Figure from V. Hirschi, R. Frederix, S. Frixione, M.V.G., F. Maltoni, R. Pittau, arXiv:1103.0621[hep-ph])

One loop-amplitudes can be determined by evaluating tree-level diagrams obtained by cutting, in all possible way, four, three, two and one of the m loop particles.

Real NLO corrections: example of additional jet production

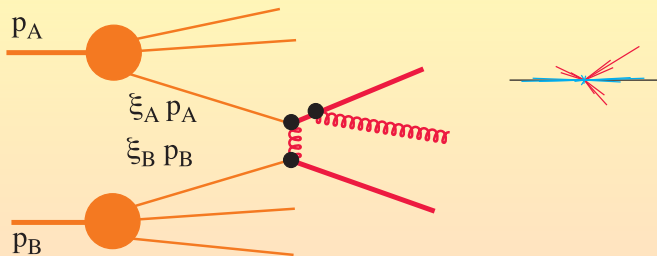


Figure: A Feynman diagram for jet production in hadron-hadron collisions. The leading order diagrams for $A + B \rightarrow jet + X$ occur at order α_s^2 . This particular diagram is for an interaction of order α_s^3 . When the emitted gluon is not soft or nearly collinear to one of the outgoing quarks, this diagram corresponds to a final state like that shown in the small sketch, with three jets emerging in addition to the beam remnants. Any of these jets can be the jet that is measured in the one jet inclusive cross section. (Figure from D. Soper, [hep-ph/9702203](https://arxiv.org/abs/hep-ph/9702203))

Real NLO corrections

- Real corrections only involve **tree-level diagrams**, so they do not require neither any additional integral nor the introduction of unitarity techniques.
- However, since **divergences** appear even in this case, a lot of work has been done concerning **subtraction schemes**, introduced to allow a 4-dim integration of the real contribution (residue/dipole/antenna subtraction). In practice,

$$\int_{n+1} d\sigma^R + \int_n d\sigma^V = \int_{n+1} (d\sigma^R - d\sigma^A)_{\epsilon=0} + \int_n (d\sigma^V + \int_1 d\sigma^A)_{\epsilon=0}$$

$d\sigma^A$ has the same singular behaviour as $d\sigma^R$

- Subtraction schemes mostly used: **Catani-Seymour method** and **FKS method**.
- Implementation in MC codes: **Helac-Dipoles** (freely available on the web), **MadFKS**, private implementations.

Combining together real and virtual contributions.

The K_{factor}

By combining together virtual and real correction contributions, i.e. the results of the MC codes used to compute them, the **infrared divergences cancel each other** (**KLN theorem** and check that the subtraction schemes work) for infrared safe observables, and one gets $d\sigma^{NLO}$.

By further integrating it over the available phase-space (specified by experimental cuts), one obtains a σ^{NLO} that can be compared to σ^{LO} , by means of the K_{factor} , defined as

$$K_{factor} \equiv \frac{\sigma^{NLO}}{\sigma^{LO}}.$$

K_{factor} values from $1/2$ up to 2 frequently appear (see e.g. phenomenological studies of $pp \rightarrow t\bar{t}b\bar{b}$).

Sometimes, even giant K_{factor} 's can show up (see recent works e.g. by M. Rubin, G.P. Salam, S. Sapeta, JHEP 09 (2010) 084)

σ^{NLO} : examples of $2 \rightarrow 4$ processes at LHC

$pp \rightarrow t\bar{t}H \rightarrow t\bar{t}b\bar{b}$ signal vs. $pp \rightarrow t\bar{t}b\bar{b}$ background

[Bevilacqua, Czakon, Garzelli, Papadopoulos, Pittau, Worek, arXiv:1003.1241[hep-ph], contribution to the LHC Higgs Cross-section Working Group]

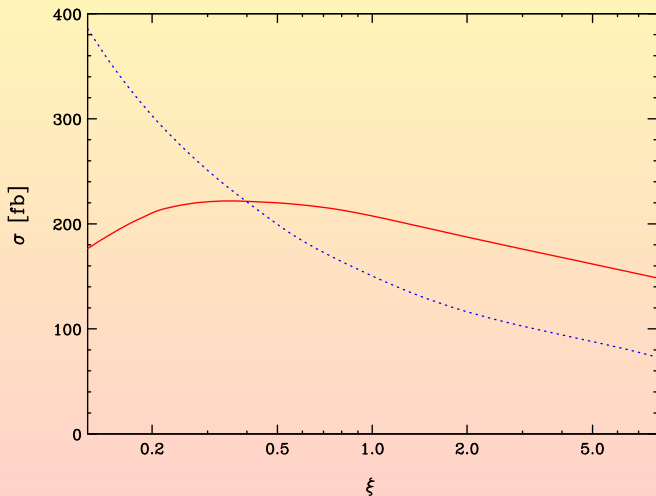
Motivation: H searches ($115 < M_H < 140\text{GeV}$) and determination of the H Yukawa couplings.

Assumptions and cuts: CTEQ6 pdf sets used consistently, $\mu_R = \mu_F = \mu_0 = M_{thr}/2$, $m_{top} = 172.6\text{ GeV}$, $m_{other\ quarks} = 0$, $m_H = 130\text{ GeV}$, H decay by narrow width approximation, recombination of b and g with $|\eta| < 5$ into jets with separation $D > 0.8$ via k_T -algorithm, phase space cuts: rapidity of the 2 (recombined) b jets $|y_b| < 2.5$ and $p_{T,b} > 20\text{GeV}$.

$$K_{signal}(\mu_0 = m_t + m_H/2) = \frac{\sigma_{signal}^{NLO}}{\sigma_{signal}^{LO}} = \frac{207.268 \pm 0.150\text{fb}}{150.375 \pm 0.077\text{fb}} = 1.38$$

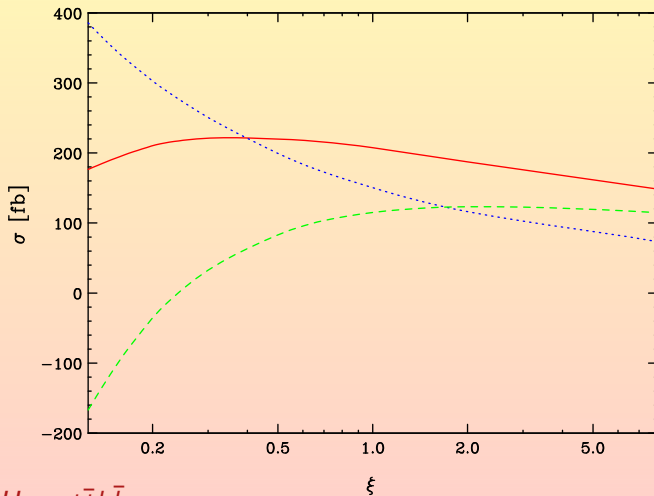
$$K_{background}(\mu_0 = m_t) = \frac{\sigma_{background}^{NLO}}{\sigma_{background}^{LO}} = \frac{2642 \pm 3\text{fb}}{1489.2 \pm 0.9\text{fb}} = 1.77$$

Signal σ^{NLO} vs σ^{LO} as a function of $\xi = \mu/\mu_0$: scale dependence attenuation....



$pp \rightarrow t\bar{t}H \rightarrow t\bar{t}b\bar{b}$

....Experimental cuts can strongly affect the result:
 effect of an additional hard jet veto $p_{T,cut} = 50\text{ GeV}$



$pp \rightarrow t\bar{t}H \rightarrow t\bar{t}b\bar{b}$
 $\sigma^{NLO} = 207.268 \pm 0.150 \text{ fb}$

$\sigma^{NLO+jet \text{ veto}} = 114.880 \pm 0.152 \text{ fb}$

Some LO and NLO σ for 4, 5, 6 leg processes

Process	μ	n_{lf}	Cross section (pb)	
			LO	NLO
a.1 $pp \rightarrow t\bar{t}$	m_{top}	5	123.76 ± 0.05	162.08 ± 0.12
a.2 $pp \rightarrow tj$	m_{top}	5	34.78 ± 0.03	41.03 ± 0.07
a.3 $pp \rightarrow tjj$	m_{top}	5	11.851 ± 0.006	13.71 ± 0.02
a.4 $pp \rightarrow tbj$	$m_{top}/4$	4	25.62 ± 0.01	30.96 ± 0.06
a.5 $pp \rightarrow t\bar{b}jj$	$m_{top}/4$	4	8.195 ± 0.002	8.91 ± 0.01
b.1 $pp \rightarrow (W^+ \rightarrow) e^+ \nu_e$	m_W	5	5072.5 ± 2.9	6146.2 ± 9.8
b.2 $pp \rightarrow (W^+ \rightarrow) e^+ \nu_e j$	m_W	5	828.4 ± 0.8	1065.3 ± 1.8
b.3 $pp \rightarrow (W^+ \rightarrow) e^+ \nu_e jj$	m_W	5	298.8 ± 0.4	300.3 ± 0.6
b.4 $pp \rightarrow (\gamma^*/Z \rightarrow) e^+ e^-$	m_Z	5	1007.0 ± 0.1	1170.0 ± 2.4
b.5 $pp \rightarrow (\gamma^*/Z \rightarrow) e^+ e^- j$	m_Z	5	156.11 ± 0.03	203.0 ± 0.2
b.6 $pp \rightarrow (\gamma^*/Z \rightarrow) e^+ e^- jj$	m_Z	5	54.24 ± 0.02	56.69 ± 0.07
c.1 $pp \rightarrow (W^+ \rightarrow) e^+ \nu_e b\bar{b}$	$m_W + 2m_b$	4	11.557 ± 0.005	22.95 ± 0.07
c.2 $pp \rightarrow (W^+ \rightarrow) e^+ \nu_e t\bar{t}$	$m_W + 2m_{top}$	5	0.009415 ± 0.000003	0.01159 ± 0.00001
c.3 $pp \rightarrow (\gamma^*/Z \rightarrow) e^+ e^- b\bar{b}$	$m_Z + 2m_b$	4	9.459 ± 0.004	15.31 ± 0.03
c.4 $pp \rightarrow (\gamma^*/Z \rightarrow) e^+ e^- t\bar{t}$	$m_Z + 2m_{top}$	5	0.0035131 ± 0.0000004	0.004876 ± 0.000002
c.5 $pp \rightarrow \gamma t\bar{t}$	$2m_{top}$	5	0.2906 ± 0.0001	0.4169 ± 0.0003
d.1 $pp \rightarrow W^+ W^-$	$2m_W$	4	29.976 ± 0.004	43.92 ± 0.03
d.2 $pp \rightarrow W^+ W^- j$	$2m_W$	4	11.613 ± 0.002	15.174 ± 0.008
d.3 $pp \rightarrow W^+ W^+ jj$	$2m_W$	4	0.07048 ± 0.00004	0.1377 ± 0.0005
e.1 $pp \rightarrow HW^+$	$m_W + m_H$	5	0.3428 ± 0.0003	0.4455 ± 0.0003
e.2 $pp \rightarrow HW^+ j$	$m_W + m_H$	5	0.1223 ± 0.0001	0.1501 ± 0.0002
e.3 $pp \rightarrow HZ$	$m_Z + m_H$	5	0.2781 ± 0.0001	0.3659 ± 0.0002
e.4 $pp \rightarrow HZ j$	$m_Z + m_H$	5	0.0988 ± 0.0001	0.1237 ± 0.0001
e.5 $pp \rightarrow Ht\bar{t}$	$m_{top} + m_H$	5	0.08896 ± 0.00001	0.09869 ± 0.00003
e.6 $pp \rightarrow Hb\bar{b}$	$m_b + m_H$	4	0.16510 ± 0.00009	0.2099 ± 0.0006
e.7 $pp \rightarrow Hj$	m_H	5	1.104 ± 0.002	1.036 ± 0.002

Table: NLO results obtained by MadLoop (virtual corrections) + MadFKS (real corrections), LO results obtained by MadGraph/MadEvent at the 7 TeV LHC (within specified cuts). The errors are due to the statistical uncertainty of Monte Carlo integration. (Figure from V. Hirschi, R. Frederix, S. Frixione, M.V.G., F. Maltoni, R. Pittau, arXiv:1103.0621 [hep-ph])

Pictorial representation of a p-p collision

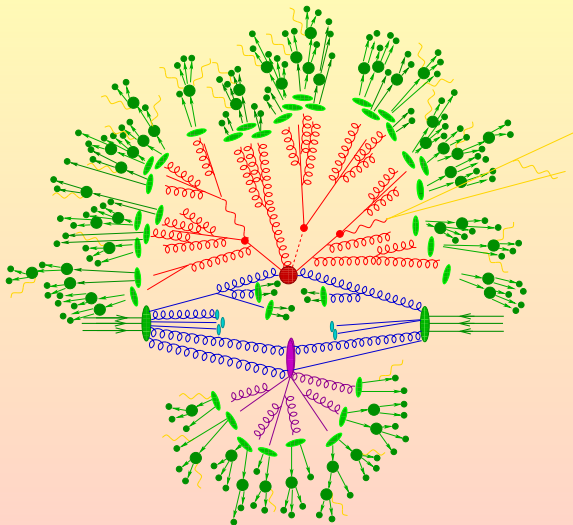


Figure: The hard interaction (big red blob) is followed by the decay of both top quarks and the Higgs boson (small red blobs). **Additional hard QCD radiation is produced (red)** and a secondary interaction takes place (purple blob) before the final-state partons hadronise (light green blobs) and hadrons decay (dark green blobs). Photon radiation occurs at any stage (yellow). (Figure taken from T. Gleisberg et al. JHEP 02 (2009), 007)

2) Parton Shower stage

- Matrix-Elements (ME) computed according to perturbation theories provide a good description of the events leading to the emission of wide-angle and high-energy particles, but fails in the description of the **small-angle and/or low-energy** emissions of each parton-parton scattering.
- Thus, the description of ME has to be supplemented by Parton Shower (PS) effects to model multiple QCD **bremstrahlung (succession of emissions, evolution from the hard-scattering scale down to low energy scales ~ 1 GeV)**. These ones are governed by factorization properties + the **Altarelli-Parisi splitting functions, universal probabilities for the splitting processes in the collinear limit**:

$$q \rightarrow qg, \quad q \rightarrow gq, \quad g \rightarrow gg, \quad g \rightarrow q\bar{q}$$

- PS provides an approximation to exact Perturbation Theory, accurate to \sim (Next to) Leading Logarithmic order (**approximate treatment of all higher order effects**).
- PS provides a **soft and collinear approximation** to the full cross-sections.
- PS evolution is encoded in the same MC generators used for the description of the hadronisation.
- PS possible ordering parameters: $k_T, \theta_{emission}$, etc.....

Merging/Matching the Parton Shower description and the Hard-Scattering description

- * It is a delicate issue!
- * At LO, the **MLM prescription** has been established as a pragmatic approach (related to the more rigorous **CKKW formalism**) and implemented in the **ALPGEN** (and **Helac**) event generators.
- * At NLO, more complicated prescriptions have to be used (due to the fact that additional jets either can appear as real radiation corrections, or can be generated by the Parton Shower algorithm). These have been implemented in approaches like **POWHEG** and **MC@NLO**, that are going to be interfaced to NLO event generators (as one of the first examples of application, see e.g. A. Kardos et al., arXiv:1102.2672[hep-ph]).
- * The aims of the prescriptions are, on the one hand, **to avoid double counting** (i.e. the same jet can not be generated in both the hard-scattering and the PS stages) and, on the other hand, **to cover all possible phase-space regions** (i.e. no dead regions and missed jets).
- * Further developments (for the future): multileg matching at NLO

Pictorial representation of a p-p collision

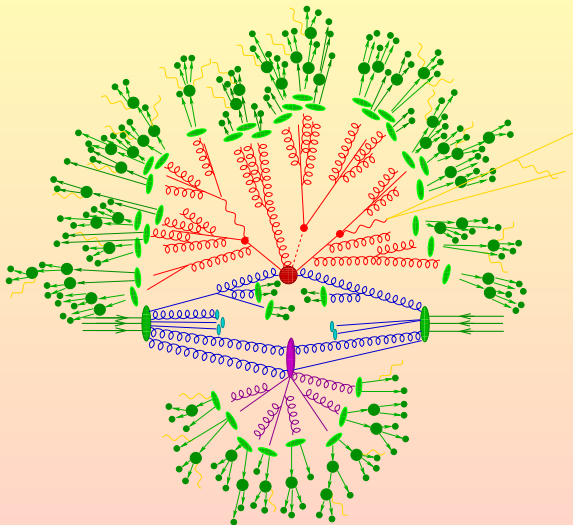


Figure: The hard interaction (big red blob) is followed by the decay of both top quarks and the Higgs boson (small red blobs). Additional hard QCD radiation is produced (red) and a secondary interaction takes place (purple blob) before the final-state partons hadronise (light green blobs) and hadrons decay (dark green blobs). Photon radiation occurs at any stage (yellow). (Figure taken from T. Gleisberg et al. JHEP 02 (2009), 007)

3) and 4): Underlying Event and Hadronisation

- The **Hadronisation** is **non-perturbative**, The **Underlying Event** can include both **non-perturbative and perturbative effects** (see e.g. the case of **multiple parton-parton interactions**).
- These two aspects are **closely related one to each other since both the “partecipant” partons and the “spectator” ones are clustered together** to give rise to final state hadrons.
- The clustering is described by means of **phenomenological models** (no elegant mathematical theory), involving a lot of **parameters**, that are adjusted in such a way to reproduce experimental data.
⇒ **Tuning** effort (recently tuning tools have been developed in order to automatize the tuning procedure, allowing to simultaneously determine the best range for many parameters).
- The parameters entering the matching between ME and PS can enter into the tuning, as well.
- New **LHC data** are quite important for better understanding the role of each of the parameters and their mutual relationship, allowing indeed to better clarify the hadronisation process, even from the theoretical point of view (reduction of the number of “free” parameters ?).

4) Hadronisation: string model vs cluster model

String models were first developed in Lund. Two partons are the extremes of **color flux tubes**. They are confined by a potential $V(r) = kr$, increasing with the distance between them ($k \sim 1 \text{ GeV/fm}$). A string **breaks** at $r = 1 - 5 \text{ fm}$, when the partons are moving apart from each other. When its invariant mass is not enough for further breakings, the string transforms, according to its mass and flavour content, in an **hadron** with a closer mass, or in a **resonance**, that subsequently decays.

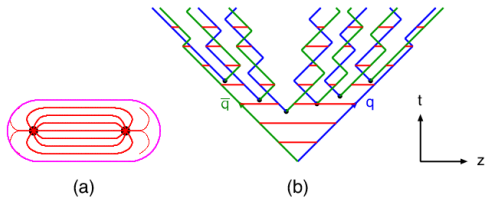


Figure: from A. Buckley et al. arXiv:1101.2599[hep-ph]

4) Hadronisation: string model vs cluster model

- **Cluster models add a pre-confinement stage**, related to the spatial properties of color connected partons. They tend to be closer in space, making clusters, that subsequently hadronize.

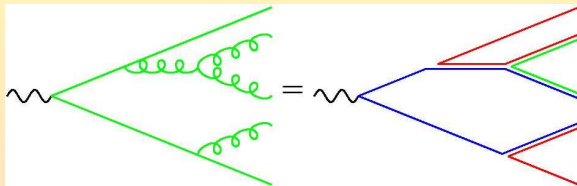


Figure: The colour structure of a parton shower to leading order in N_c is planar. In the limit $N_c \rightarrow \infty$ non-planar configurations are suppressed. (Figure from A. Buckley et al. arXiv:1101.2599[hep-ph])

- The starting point of cluster models is the $g \rightarrow q\bar{q}$ splitting (**color connection representation**).
- Disadvantage of both the string and cluster models: **strings (clusters) evolve independently one from each other** (not good in multiple interaction and dense matter conditions, where collective effects may occur).

MC tools available: PYTHIA, HERWIG, HERWIG++

- **PYTHIA** has been developed by T. Sjostrand (Lund) and collaborators since many years. It is the oldest and most widely used PS and hadronisation tool. It was originally written in Fortran. Nowadays, a C++ version is available and under continuous development. It is a refined **string** model, widely used for data analysis at colliders. Good reproduction of experimental data, thanks to many years of tuning.
- **HERWIG** and **HERWIG++** have a more complicated history. Many recent progresses on them. The theoreticians are encouraging the use of **cluster** models, since they are well founded (the invariant mass distribution of clusters is asymptotically universal) and **only a few parameters enter these models as compared to string models** (the most important one is the shower cut-off scale Q_0).
- Other hadronisation codes are also available, e.g. the **SHERPA** dedicated module (cluster model).

⇒ The results of a MC event generator can differ, according to the hadronisation module used!

h - h total cross-section

- **elastic component**: all reactions where the only exchanged quantity is momentum (the particle identity and all other quantum numbers remain the same).
- **inelastic component**: all the rest. This includes:
 - **diffractive events**: they can involve a single beam, both beams (double), or the central region of the collision, where decays of an excited system occur. A diffractive event is characterized and identified in practice by the presence of one or more rapidity gaps.
 - **non-diffractive events**

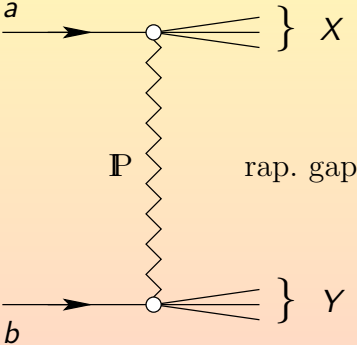
$$\sigma_{TOT} = \sigma_{ELASTIC} + \sigma_{INELASTIC}$$

$$\sigma_{INELASTIC} = \sigma_{DIFFRACTIVE} + \sigma_{NON-DIFFRACTIVE}$$

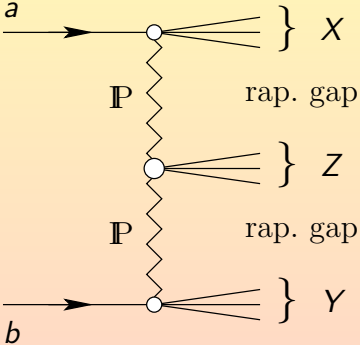
$$\sigma_{DIFFRACTIVE} = \sigma_{SINGLEDIFF} + \sigma_{DOUBLEDIFF} + \sigma_{CENTRALDIFF}$$

Diffractive events are of primary interest for the **cosmic ray** community, but are **the hardest to be measured at colliders**, since forward coverage is needed (for central diff. prod. at Tevatron and LHC, see e.g. L.A. Harland-Lang et al., arXiv:1101.1420[hep-ph])

Example of diffractive processes



(a)



(b)

Figure: Processes with (a) one and (b) two large rapidity gaps. (Figure from O. Nachtmann, hep-ph/0312279)

h-h interactions: recipes from the cosmic ray community

- The cosmic ray community is, even from an historical point of view, mainly interested in the study of the **soft** component of **h - h** interactions.
- One of the theories first developed at this aim was the **DPM** based on **reggeon and pomeron exchange**.
- This theory relies on **unitarity to relate elastic and inelastic scattering** processes through the optical theorem. **Regge Theory** is a pre-QCD approach.
- In DPM two hadrons interact by exchanging one or more reggeons (each one equivalent to a $q\bar{q}$ pair) or pomerons, closed loop excitations (each one equivalent to a gg pair) that are color-singlet. Both soft and (semi-)hard pomerons were introduced.
- (3-dim vision because this model describe h-h interactions \neq 2-dim vision offered by Feynman diagrams, that instead describe point-like elementary parton-parton interactions).
- A cascade of partons originates from pomeron cuts. **Each pomeron cut leads to two chains**, each one corresponding to a gluon included in the pomeron.
- **Multiple interactions** are possible, each of them corresponding to a different pomeron exchange.

A pictorial view of pomeron exchange

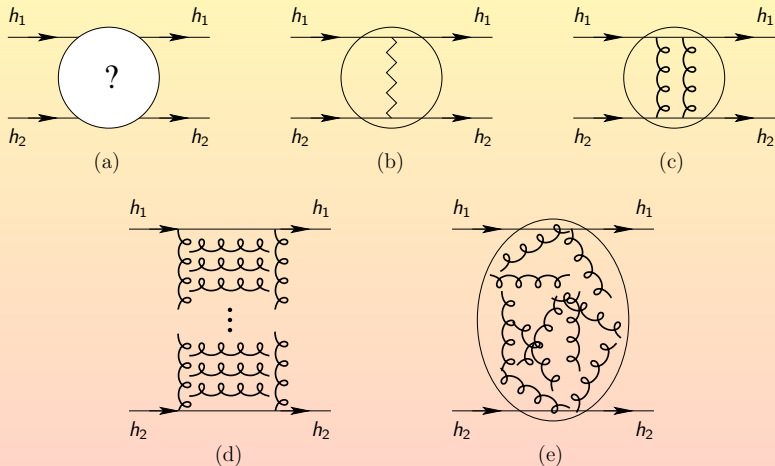
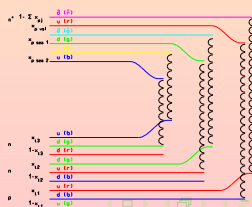
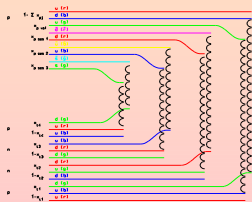


Figure: Hadron-hadron scattering: (a) what happens?, (b) phenomenological pomeron and (c) two gluon exchange, (d) exchange of a reggeised gluon ladder and (e) in the fluctuating vacuum gluon field. (Figure from O. Nachtmann, hep-ph/0312279)

String formation and fragmentation

Strings stretch out between fermions of different colors (in such a way that each chain is overall colorless) (see the Lund model). As soon as the partons move apart one from each other, the string becomes more and more stretched, up to breaking up. In the breaking point, new partons of opposite colors appear at the end of the two resulting chains. These ones are allowed to evolve in a similar way, up to the stage in which all chains have not enough energy to break up and each of them hadronizes. Due to the fact that mesons ($q\bar{q}$) and baryons (made by 3 quarks or 3 antiquarks) exist in nature, while each chain has only two ends, chains can stretch out between quarks and antiquarks, and between quarks (antiquarks) and di-quarks (or anti-di-quarks).



Implementation of these concepts: the DPMJET code

The formalism of pomeron exchange was implemented in the [DPMJET](#) code, used in both accelerator and cosmic ray physics.

- [DPMJET-II](#) J. Ranft, Phys. Rev. D **51** (1995), 64
- [DPMJET-III](#) S. Roesler, R. Engel and J. Ranft, hep-ph/0012252

[DPMJET](#) has been used **in the analysis of the first LHC data**, last year. **Key-point** allowing its use at LHC: it includes hard pomeron effects and it provides a **smooth transition between hard and soft collision** events.

h - A and **A - A** collisions are described in [DPMJET](#) by the same concepts used for **h - h** interactions, supplemented by the **Glauber-Gribov formalism** for treating **nuclear effects**.

DPMJET @ LHC: some examples

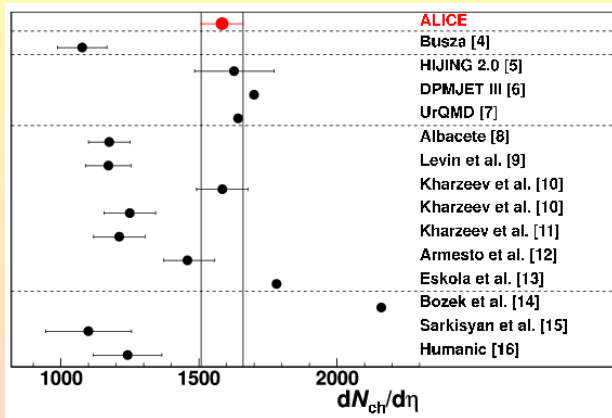


Figure: Charged-particle pseudo-rapidity density at mid-rapidity in Pb - Pb collisions at $\sqrt{s_{NN}} = 2.76 \text{ TeV}$, for the most central 5% fraction of the hadronic cross section. Experimental results provide a constraint for models describing high-energy A - A collisions. (Figure from the Alice Collaboration, PRL 105, (2010) 252301)

The all-particle flux of Cosmic Rays

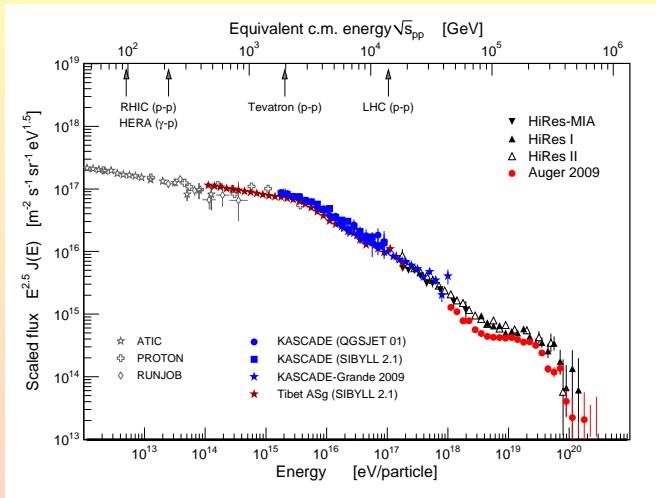


Figure: A compilation of measurements of the all-particle spectrum of cosmic rays. Figure from R. Engel in arXiv:1101.1852[hep-ex]. See also J. Blumer et al. Prog. Part. Nucl. Phys. 63 (2009) 293–338.

DPMJET use in Cosmic Ray Physics

- It is among the high-energy models available in the **CORSIKA** package (the others are **QGSJET**, **QGSJET-II**, **EPOS**, **NEXOS**, **SIBYLL**, etc....). These models are based on (slightly) different formalisms (e.g. in the treatment of diffraction). In all cases **many parameters** are present, whose values are fixed at low energies on the basis of experimental data and extrapolated at higher energies.
- **DPMJET** is used for describing **$h - A$** and **$A - A$** interactions at high-energy, in the **FLUKA** multipurpose transport and interaction code (not only for **Cosmic Ray Physics** simulations and their application to **Space Physics** and Radioprotection, but also for **beam line** and **detector design**).

The FLUKA collaboration

Main historical developers: A. Fassò, A. Ferrari, J. Ranft, P.R. Sala

Present developers (including both modelling and software experts and advanced users):

Giuseppe BATTISTONI¹, Francesco BROGGI¹, Markus BRUGGER², Mauro CAMPANELLA¹, Massimo CARBONI⁵, Anton EMPL¹⁰, Alberto FASSO³, Ettore GADIOLI¹, Francesco CERUTTI², Alfredo FERRARI², Anna FERRARI¹⁴, Maria Vittoria GARZELLI¹⁵, Mattias LANTZ¹³, Andrea MAIRANI¹, Annarita MARGIOTTA⁸, Cristina MORONE⁷, Silvia MURARO¹, Katia PARODI⁹, Vincenzo PATERA⁶, Maurizio PELLICIONI⁶, Lawrence PINSKY¹⁰, Johannes RANFT⁴, Stefan ROESLER², Sofia ROLLET¹², Paola R. SALA¹, Mario SANTANA³, Lucia SARCHIAPONE⁵, Massimiliano SIOLI⁸, George SMIRNOV², Florian SOMMERER⁹, Christian THEIS², Stefania TROVATI², Rosaria VILLARI⁶, Heinz VINCKE², Helmut VINCKE², Vasilis VLACHOUDIS², Joachim VOLLAIRE², Neil ZAPP¹¹

¹INFN, Milano, Italy ²CERN, Geneva, Switzerland ³SLAC, Stanford, U.S.A. ⁴University of Siegen, Siegen, Germany ⁵INFN, Legnaro, Italy ⁶INFN, Frascati, Italy ⁷INFN and University of Roma II, Roma, Italy ⁸INFN and University Bologna, Bologna, Italy ⁹HIT, Heidelberg, Germany ¹⁰University of Houston, Houston, U.S.A. ¹¹NASA, Houston, U.S.A. ¹²ARC Seibersdorf, Seibersdorf, Austria ¹³Uppsala University, Uppsala, Sweden ¹⁴FZD Dresden-Rossendorf, Dresden, Germany ¹⁵INFN, Italy and University of Granada, Spain

FLUKA is available on the web at <http://www.fluka.org>

Last release in March 2011 (respin April 2011)

It is continuously developed and maintained according to an **INFN-CERN agreement**, active since 2002.

Hadronic interactions in FLUKA

- **h - h**
 - Low energy **h - h**: elastic scattering (including charge exchange)
 - Intermediate energy **h - h** (i.e. above resonance prod. threshold): isobar model, describing resonance production and decay
 - High energy **h - h**: in-house implementation of **DPM** ($E > 3 - 5$ GeV)
- **h - A**
 - Low energy **h - A**: refined **GINC** (on the basis of low energy **h - h** + Pre-Equilibrium + Coalescence, all embedded in the **PEANUT** module)
 - Higher energy **h - A** ($E > 5$ GeV): **DPMJET**, nowadays in alternative to the **PEANUT-GINC** extension.
- **A - A**
 - Low energy **A - A**: **BME** ($E < 100$ MeV/A)
 - Intermediate energy **A - A**:
 - in-house QMD (20 MeV/A $< E < 600$ MeV/A)
 - modified version of **RQMD2.4** (H. Sorge et al.) ($100 - 200$ MeV/A $< E < 5$ GeV/A)
 - High-energy **A - A**: **DPMJET-II** or **DPMJET-III** ($E > 5$ GeV/A)

Important: all these modules are interfaced to the FLUKA fragmentation/evaporation/fission/Fermi break-up + γ de-excitation module, which provides a common framework to describe the fate of the reaction products. This is a **unique feature** of **FLUKA**, providing a refined description of low energy effects.

Use of FLUKA in Cosmic Ray Physics

- A restricted but up-to-date sub-library of **FLUKA** can be used in the **CORSIKA** package as a **low energy model** (providing an **alternative to GHEISHA**, for $E < 200$ GeV/A).
- **FLUKA** can be used **standalone** (superposition model) or **interfaced to DPMJET-II or III** to describe **A - A** interactions (up to GCR primary energies $\sim 10^{15} - 10^{16}$ eV).
 - Examples of its **use for the study of GCR interactions**:
 - G. Battistoni et al., hep-ph/0612075
 - G. Battistoni et al., arXiv:0711.2044[astro-ph]
 - G. Battistoni et al., arXiv:1002.4655[hep-ph]
 - **FLUKA** has been used for CR studies even by the OPERA collaboration, see EPJC 67 (2010), 25.
 - Examples of its **use in Cosmic Ray applicative problems (civil flight and space radioprotection)**:
 - G. Battistoni et al., Rad. Prot. Dos. 112 (2004), 331
 - F. Ballarini et al., Adv. Space Res. 37 (2006), 1791

Some results concerning μ charge ratio

- The **L3 + COSMIC** experiment provides μ^+/μ^- data as a function of p_μ , up to 1 TeV, and of the **azimuthal angle**. The **FLUKA** predictions agree with the data, at all angles.
- The **MINOS** experiment provides μ^+/μ^- as a function of E_μ in the energy range $1 \text{ TeV} < E_\mu < 7 \text{ TeV}$. The **FLUKA** predictions slightly underestimate the data by $\sim 3\%$.

Some results concerning μ charge ratio

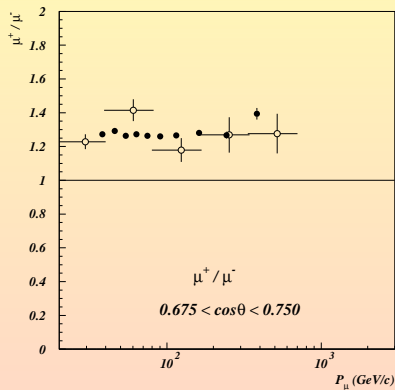
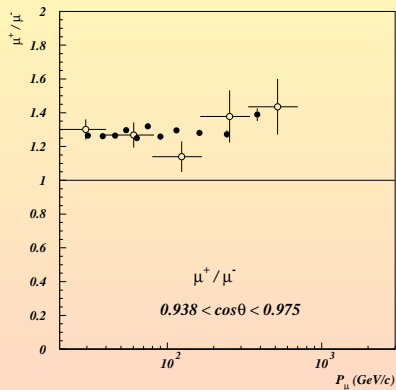


Figure: L3+C (black filled circles) vs FLUKA (empty circles), simulations by S. Muraro, Ph.D. Thesis, Milano

Some results concerning μ charge ratio

- The **L3 + COSMIC** experiment provides μ^+/μ^- data as a function of p_μ , up to 1 TeV, and of the **azimuthal angle**. The **FLUKA** predictions agree with the data, at all angles.
- The **MINOS** experiment provides μ^+/μ^- as a function of E_μ in the energy range $1 \text{ TeV} < E_\mu < 7 \text{ TeV}$. The **FLUKA** predictions slightly underestimates the data by $\sim 3\%$.

Possible reasons of the discrepancy:

- **FLUKA** underestimates **K** production and/or overestimates π production ?
- **K** production in **FLUKA** has been validated only up to **400 GeV** and over a very restricted forward region (during the project/validation of the CNGS ν beam)
- Primary spectrum composition ?

Some results concerning μ charge ratio: most recent data confirm the old ones

- The **CMS** experiment provides μ^+/μ^- data as a function of p_μ in the range $10 \text{ GeV}/c < p_\mu < 1 \text{ TeV}$. At present, this can be considered the most comprehensive measurement of μ charge ratio, since this experiment is sensitive to both low energy and high-energy μ . Angular dependence of data is not reported in first publications. The **FLUKA** predictions agree with the data.
- The **ALICE** experiment provides μ^+/μ^- data as a function of p_μ at higher energies with respect to CMS ($p_\mu > 100 \text{ GeV}/c$). The difficulty to use ALICE to detect lower energy μ is due to the low magnetic field of this experiment. **FLUKA** predictions still to be compared with the data.....
- The **OPERA** experiment, located at the Gran Sasso laboratory, provides a complementary measure of μ^+/μ^- . Due to its location, under 1.5 Km of rocks, it is sensitive to high-energy μ . Interpretation of its data is still controversial.

Some results concerning μ charge ratio

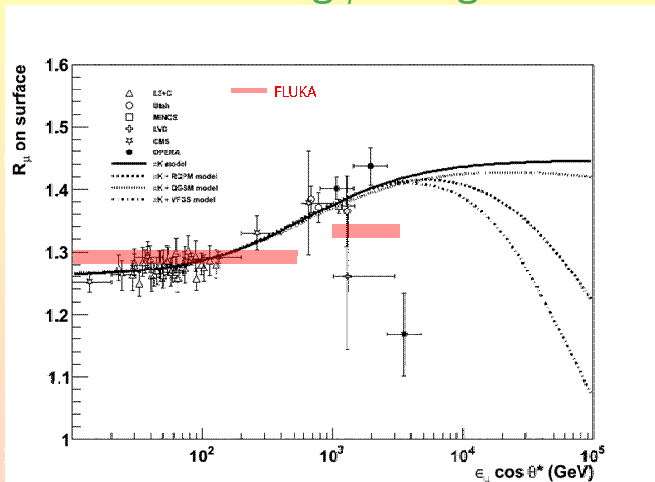


Figure: μ^+/μ^- charge ratio as a function of the surface energy $E_\mu \cos \theta$: results of the FLUKA simulation (each of the two pink bands represents an average value of the charge ratio over all $E_\mu \cos \theta$ values in the corresponding abscissa interval) vs. experimental data (Utah, LVD, L3+C, MINOS, CMS and OPERA). (Figure from G. Battistoni, M.V.G., A. Margiotta, S. Muraro, M. Sioli for the FLUKA Collab., arXiv:1101.1852[hep-ex])

Some results concerning μ underground

- The measure of the shape of muon lateral distribution in **experiments deep underground** allows the study of the **transverse structure of hadronic interactions**.
- In fact these experiments, due to the overburden, are **only sensitive to high-energy muons** ($E > TeV$).
- **Decoherence function = distribution of the distance between μ pairs in a bundle**

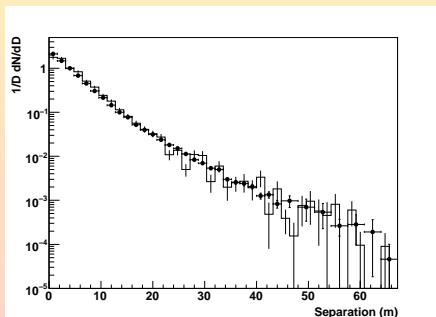


Figure: Decoherence distribution of μ pairs in a bundle (histogram: FLUKA + DPMJET simulation; symbols: MACRO data) (Figure from G. Battistoni, M.V.G., A. Margiotta, S. Muraro, M. Sioli for the FLUKA Collab., arXiv:1101.1852[hep-ex])

Air shower development

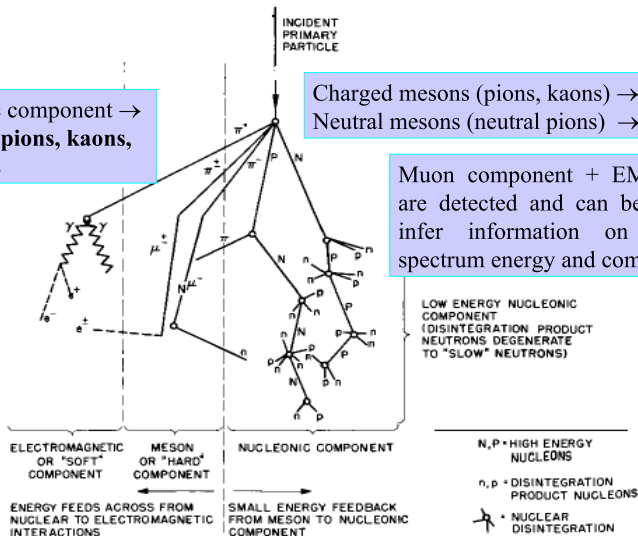
Primary interaction in the upper atmosphere

→ Hadronic Shower

Hadronic component →
**charged pions, kaons,
nucleons**

Charged mesons (pions, kaons) → **Muons**
Neutral mesons (neutral pions) → **Photons**

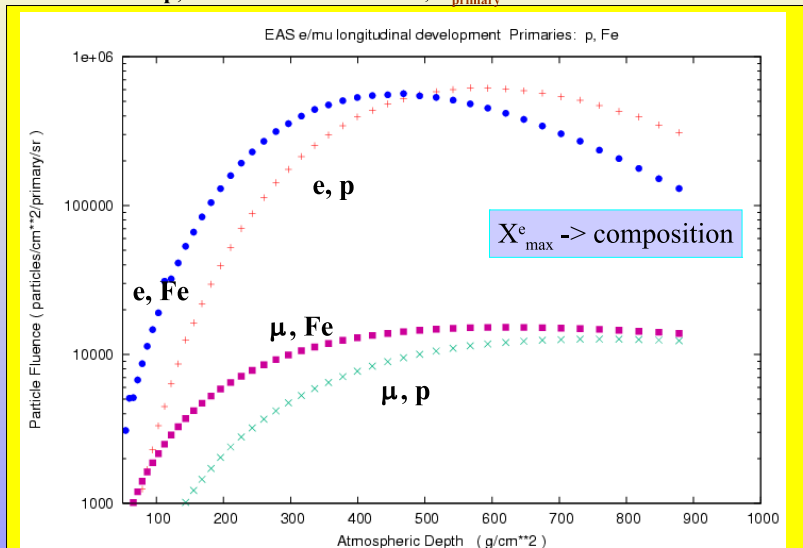
Muon component + EM shower
are detected and can be used
to infer information on primary
spectrum energy and composition



Some results concerning air shower development

e/μ fluence as a function of the atmospheric depth

p, Fe + Air vertical shower, $E_{\text{primary}} = 10^{15}$ eV



Some results concerning air shower development

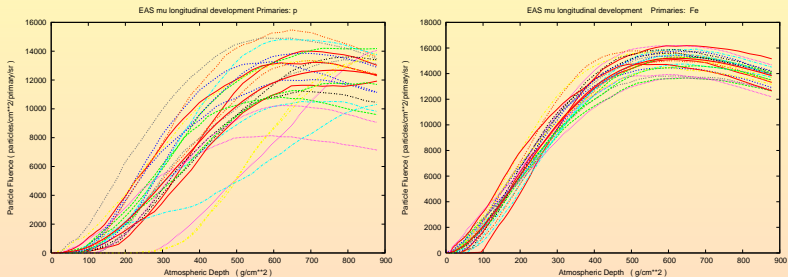


Figure: μ fluence as a function of the atmospheric depth for vertical showers induced by p (left panel) and Fe (right panel) primaries with 10^{15} eV energy. Each line in each figure is the result for a different shower. In case of p showers, the development of the hadronic component shows larger **fluctuations**, also related to the depth of the first interaction. (Figure from G. Battistoni, M.V.G., E. Gadioli et al., hep-ph/0612075)

Some results concerning air shower development

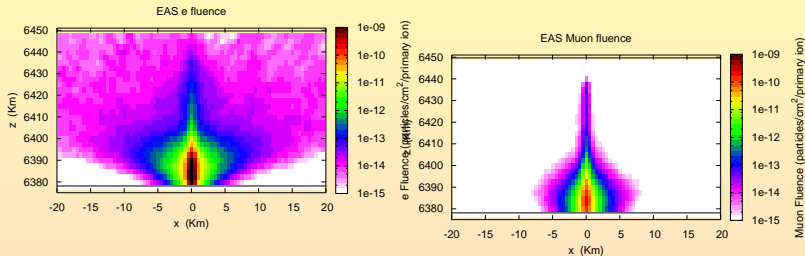
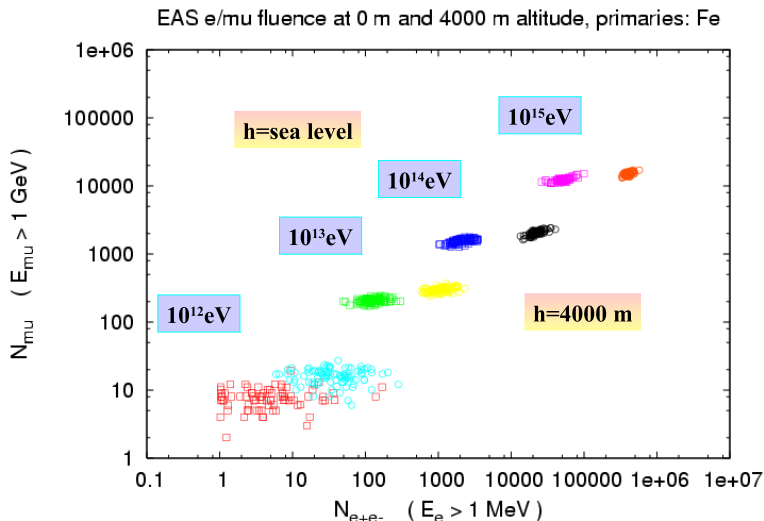


Figure: Spatial distribution of e fluence (left panel) and μ fluence (right panel) (particles/cm²/primary) for vertical showers induced by Fe primaries with 10^{15} eV energy. The results are obtained as an average over ~ 100 events for each energy. The primaries come from the top of the atmosphere (top of each figure) and propagate towards the Earth's surface located at ~ 6378 km with respect to the Earth's center. (Figure from G. Battistoni, M.V.G., E. Gadioli et al., hep-ph/0612075)

- e lateral spread due to multiple Coulomb scattering
- μ lateral spread due to p_T distribution of charged π and K

Some results concerning air shower development

(N_e, N_μ) correlation, Fe + Air : dependence on the altitude



Some work in progress

- Use of LHC results to further constrain FLUKA and DPMJET.
- See the work by D. d'Enterria et al., arXiv:1101.5596[hep-ph], on CORSIKA models: a similar work can be done on FLUKA, FLUKA+DPMJET.

Summary and Conclusions

- We have shown an **overview over hadronic interactions and their modelization**, by discussing both their hard and their soft component, and MC models for their evaluation.
- The **transition region** (from hard to soft) has to be modelled with attention (see **DPMJET**).
- The **gap between the Particle Physics community and the Cosmic Ray Physics community** is still far from being filled, even if some recent attempts deserve attention (see e.g. the recent ECT* Workshop on h - h and Cosmic Ray Interactions at multi-TeV Energies , last winter).
- The **participation of cosmic ray physicists to the analysis of LHC data will help to further reduce this gap**, since LHC data can be used to further constrain present hadronisation and hadronic interaction models used in Cosmic Ray Physics studies.
- Even **data from astroparticle physics experiments**, like OPERA and MACRO, can help at this purpose, by providing **complementary information**.
- All LHC signals detected so far have been associated to SM particles. However, **if new particles exist, their degrees of freedom will have to be incorporated** both in the MC codes for data analysis at LHC (so far only a few of them, e.g. **LO MadGraph/MadEvent**, **SHERPA**, include **Physics BSM**), and in the MC codes for Cosmic Ray Shower analyses.

Acknowledgements

In this seminar results have been presented obtained **thanks to the co-operation with**

- the **HELAC-NLO collaboration** (G. Bevilacqua, M. Czakon, P. Draggiotis, A. van Hameren, I. Malamos, C.G. Papadopoulos, R. Pittau and M. Worek) → Physics at colliders
- the **MadLoop collaboration** (V. Hirschi, R. Frederix, S. Frixione, F. Maltoni, R. Pittau) → Physics at colliders
- the **FLUKA collaboration** (in particular, G. Battistoni, A. Margiotta, S. Muraro, J. Ranft, S. Roesler and M. Sioli) → Cosmic Ray Physics.

Suggested reviews for further reading:

- * A. Buckley et al., arXiv:1101.2599[hep-ph].
- * L.A. Anchordoqui, arXiv:1104.0509[hep-ph].